

Exact Calculation of Pair Production

INGJALD ØVERBØ, KJELL J. MORK, AND HAAKON A. OLSEN

Institute of Physics, University of Trondheim (NLHT), Trondheim, Norway

(Received 22 July 1968)

Positron spectra and total cross sections for pair production in the field of an atom are calculated for a range of values of the atomic number and for photon energies below about 2.5 MeV. Screening effects by the atomic electrons are neglected. Good agreement with earlier theoretical calculations and with available experimental results is obtained.

I. INTRODUCTION

EXACT calculations of the pair production and bremsstrahlung cross sections beyond the first-order Born approximation of Bethe and Heitler have, until now, only been available for high energies,¹ and for bremsstrahlung for nonrelativistic energies.² For the case of pair production for photon energies below 5 MeV, where it is well known from experiments that large deviations from the Bethe-Heitler formula are to be expected, theoretical cross sections are available for only a few elements and energies.^{3,4}

In the present paper, the exact positron spectrum and total pair-production cross section is calculated for a range of values of the atomic number Z and for photon energies from threshold to about 2.5 MeV.

II. CROSS SECTIONS

The differential bremsstrahlung cross section is given by

$$d\sigma = [1/(2\pi)^4](r_0^2/\alpha)(\epsilon_1/p_1)p_2\epsilon_2kdkd\Omega_kd\Omega_2|H_B|^2, \quad (1)$$

where $r_0 = e^2/mc^2$, $\alpha = e^2/\hbar c$, k is the photon energy, and ϵ_1 , \mathbf{p}_1 and ϵ_2 , \mathbf{p}_2 are the initial- and final-state energies and momenta of the electron. Energies are measured in units of the electron rest energy mc^2 and momenta in units of mc .

The matrix element H_B is given by

$$H_B = \int d^3x \bar{\Phi}_-(\mathbf{p}_2, \zeta_2, \mathbf{r}) \gamma \cdot \mathbf{e}^* e^{-i\mathbf{k} \cdot \mathbf{r}} \Phi_+(\mathbf{p}_1, \zeta_1, \mathbf{r}), \quad (2)$$

where the initial- and final-state electron wave functions in the atomic field, $\Phi_+(\mathbf{p}_1, \zeta_1, \mathbf{r})$ and $\Phi_-(\mathbf{p}_2, \zeta_2, \mathbf{r})$, have asymptotic forms: plane wave plus spherical outgoing and ingoing waves, respectively. The electron polarization four-vectors for initial and final states are denoted by ζ_1 and ζ_2 respectively, and the photon momentum and polarization are denoted by \mathbf{k} and \mathbf{e} .

¹ H. A. Bethe and L. C. Maximon, Phys. Rev. **93**, 768 (1954); H. Davies, H. A. Bethe, and L. C. Maximon, *ibid.* **93**, 788 (1954).

² A. Sommerfeld, Ann. Physik **11**, 257 (1931).

³ J. C. Jaeger and H. R. Hulme, Proc. Roy. Soc. (London) **148**, 708 (1935); **153**, 443 (1936).

⁴ J. C. Jaeger, Nature **137**, 781 (1936); **148**, 86 (1941).

The differential pair-production cross section is obtained from bremsstrahlung in the usual way:

$$d\sigma = [1/(2\pi)^4](r_0^2/\alpha)(1/k)p_+\epsilon_+p_-\epsilon_-d\epsilon_+d\Omega_+d\Omega_-|H_p|^2, \quad (3)$$

where the matrix element H_p is obtained from H_B , Eq. (2), by the substitutions $\mathbf{p}_1 \rightarrow -\mathbf{p}_+$, $\epsilon_1 \rightarrow -\epsilon_+$, $\zeta_1 \rightarrow -\zeta_+$, $\mathbf{k} \rightarrow -\mathbf{k}$, $\omega \rightarrow -\omega$, $\mathbf{e} \rightarrow \mathbf{e}^*$, $\mathbf{p}_2 \rightarrow \mathbf{p}_-$, $\epsilon_2 \rightarrow \epsilon_-$, and $\zeta_2 \rightarrow \zeta_-$, where $+$ and $-$ designate positron and electron quantities, respectively. In this way, one obtains

$$H_p = \int d^3x \bar{\Phi}_-(\mathbf{p}_-, \zeta_-, \mathbf{r}) \gamma \cdot \mathbf{e} e^{i\mathbf{k} \cdot \mathbf{r}} \Phi_+(\mathbf{p}_+, -\zeta_+, \mathbf{r}). \quad (4)$$

It is to be noted that the positron wave function contains asymptotically spherical ingoing waves, as the substitutions $\epsilon_1 \rightarrow -\epsilon_+$ and $\mathbf{p}_1 \rightarrow -\mathbf{p}_+$ (but $|\mathbf{p}_1| \rightarrow |\mathbf{p}_+|$) change outgoing into ingoing spherical waves.

The wave functions in the spherically symmetric atomic field may be written most transparently in the form

$$\Phi_{\pm}(\mathbf{p}, \zeta, \mathbf{r}) = \left(\frac{\epsilon+1}{2\epsilon}\right)^{1/2} \sum_{l,j} i^l e^{\pm i\delta_{lj}} \begin{pmatrix} 1 \\ -i(\epsilon-V+1)^{-1} \boldsymbol{\sigma} \cdot \nabla \end{pmatrix} \times g_{lj}(r) [|\kappa| P_l(\cos\theta) - i(\kappa/|\kappa|) P_l^1(\cos\theta) \boldsymbol{\sigma} \cdot \mathbf{n}] v(\zeta), \quad (5)$$

with $\cos\theta = \mathbf{p} \cdot \mathbf{r}/pr$, which is equivalent to Darwin's solution^{5,6} of the Dirac equation. Here l and j are the orbital angular momentum and total angular momentum quantum numbers, respectively, δ_{lj} is the phase shift, V is the potential energy of the electron in the atomic field, P_l and P_l^1 are Legendre polynomials, $g_{lj}(r)$ is the radial wave function, and κ is defined by

$$\kappa = l(l+1) - j(j+1) - \frac{1}{4}, \quad (6)$$

or $\kappa = -(l+1)$ for $j = l + \frac{1}{2}$ and $\kappa = l$ for $j = l - \frac{1}{2}$. The unit vector \mathbf{n} is given by

$$\mathbf{n} = \mathbf{p} \times \mathbf{r} / |\mathbf{p} \times \mathbf{r}| \quad (7)$$

⁵ C. G. Darwin, Proc. Roy. Soc. (London) **A118**, 654 (1928).

⁶ For a direct proof of Eq. (5), see H. A. Olsen, *Applications of Quantum Electrodynamics, Springer Tracts in Modern Physics* (Springer-Verlag, Berlin, 1968), Vol. 44.

and $v(\zeta)$ is the free-particle Pauli two-component spinor defined as the state with polarization ζ ,

$$\sigma \cdot \zeta v(\zeta) = v(\zeta). \tag{8}$$

The normalization of Φ_{\pm} is chosen in such a way that for a plane wave ($V=0$), the wave function has the form

$$\Phi_0 = \left(\frac{\epsilon+1}{2\epsilon}\right)^{1/2} \begin{pmatrix} 1 \\ \sigma \cdot \mathbf{p} / (\epsilon+1) \end{pmatrix} e^{i\mathbf{p} \cdot \mathbf{r}} v(\zeta). \tag{9}$$

This result is easily obtainable from Eq. (5) by setting $V=0$, which implies that $\delta_{ij}=0$ and $g_{ij}(\mathbf{r})=j_i(\mathbf{p}\mathbf{r})$, $j_i(\mathbf{p}\mathbf{r})$ being the spherical Bessel function.

The radial wave function $g_{ij}(\mathbf{r})$ satisfies the wave equation

$$\frac{d^2}{dr^2} g_{ij} + \frac{2}{r} \frac{dg_{ij}}{dr} + \left\{ (\epsilon - V)^2 - 1 - \frac{l(l+1)}{r^2} \right\} g_{ij} + \frac{dV}{dr} (\epsilon - V + 1)^{-1} \left(\frac{dg_{ij}}{dr} + \frac{\kappa+1}{r} g_{ij} \right) = 0. \tag{10}$$

For a pure Coulomb potential the well-known solution is⁷

$$g_{ij}(\mathbf{r}) = \frac{(2\mathbf{p}\mathbf{r})^{\gamma-1} e^{\pi\eta/2} |\Gamma(\gamma+iy)|}{\Gamma(2\gamma+1)} (\Phi + \Phi^*), \tag{11}$$

where

$$\Phi = e^{-i\mathbf{p}\mathbf{r} + i\eta(\gamma+iy)} F(\gamma+1+iy, 2\gamma+1, 2i\mathbf{p}\mathbf{r}), \tag{12}$$

with F the confluent hypergeometric function, where

$$A_{\kappa_+ \kappa_- M} = f_{\kappa_+ \kappa_-} \sum_{L=L_{\min}}^{L_{\max}} (-1)^{(L-L_{\min})/2} \sum_{n=0}^L \frac{(L+n)!}{n!(L-n)!} \left(\frac{1}{2k}\right)^n \frac{\Gamma(a)}{(k+p_++p_-)^a} \times \left[\left[(\epsilon_++1)(\epsilon_+1) \right]^{1/2} \left(\frac{(\kappa_+-M)(\kappa_--M)}{(2\kappa_+-1)(2\kappa_++1)} \right)^{1/2} V(l_- L_+ 'M) R^+_{\kappa_+ \kappa_-} - \left[(\epsilon_+-1)(\epsilon_--1) \right]^{1/2} \left(\frac{(\kappa_++M)(\kappa_--M)}{(2\kappa_++1)(2\kappa_--1)} \right)^{1/2} V(l_- 'L_+ M) R^-_{\kappa_+ \kappa_-} \right],$$

with

$$f_{\kappa_+ \kappa_-} = \frac{(2p_+)^{\gamma_+-1/2} (2p_-)^{\gamma_--1/2} e^{(\pi/2)(\gamma_++\gamma_-)} |\Gamma(\gamma_++iy_+)| |\Gamma(\gamma_--iy_-)|}{\Gamma(2\gamma_++1) \Gamma(2\gamma_--1)},$$

$$V(l_- L_+ 'M) = (2L+1) \left(\frac{2L+1}{2l_+'+1} \right)^{1/2} C_{l_- L}(l_+'0; 00) C_{l_- L}(l_+'M; M0),$$

and

$$R^{\pm}_{\kappa_+ \kappa_-} = \text{Im} \left\{ e^{-i(\pi/2)(\gamma_++\gamma_--L-1)} [K_+ K_- F_2(a; b_+, b_-; c_+, c_-; x_+, x_-) \pm K_+ K_-^* F_2(a; b_+, b_- - 1; c_+, c_-; x_+, x_-) \mp K_+^* K_- F_2(a; b_+ - 1, b_-; c_+, c_-; x_+, x_-) - K_+^* K_-^* F_2(a; b_+ - 1, b_- - 1; c_+, c_-; x_+, x_-)] \right\},$$

$$\gamma_{\pm} = Z\alpha\epsilon_{\pm}/p_{\pm}, \quad \gamma_{\pm} = [\kappa_{\pm}^2 - (Z\alpha)^2]^{1/2}, \quad l_{\pm} = \kappa_{\pm}, \quad \kappa_{\pm} > 0 \quad l_{\pm}' = \kappa_{\pm} - 1, \quad \kappa_{\pm} > 0 \\ = -\kappa_{\pm} - 1, \quad \kappa_{\pm} < 0, \quad = -\kappa_{\pm}, \quad \kappa_{\pm} < 0,$$

$$a = \gamma_+ + \gamma_- - n, \quad b_{\pm} = \gamma_{\pm} + iy_{\pm} + 1, \quad c_{\pm} = 2\gamma_{\pm} + 1, \quad K_{\pm} = (\gamma_{\pm} + iy_{\pm}) e^{i\eta_{\pm}},$$

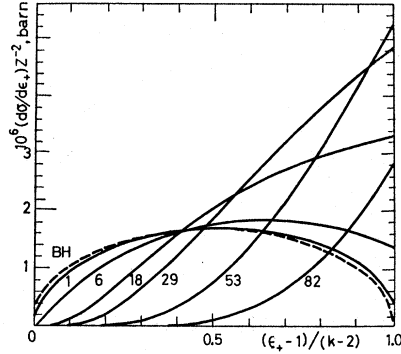


FIG. 1. Positron spectrum for a photon energy of 1.073 MeV ($k=2.10$). The curve marked BH gives the Bethe-Heitler spectrum. The numbers attached to the curves give the atomic number of the target element.

$\gamma = [\kappa^2 - (Z\alpha)^2]^{1/2}$, $y = Z\alpha\epsilon/p$, and η defined by

$$e^{2i\eta} = -\frac{\kappa - iy/\epsilon}{\gamma + iy}.$$

The normalization of g_{ij} is such that, for large values of r ,

$$g_{ij} = (1/p\mathbf{r}) \sin(p\mathbf{r} - \frac{1}{2}l\pi + \delta_{ij}).$$

With wave functions of this form, we find the positron spectrum

$$\frac{d\sigma}{d\epsilon_+} = r_0^2 \frac{2}{\alpha k^3} \sum_{\kappa_+ \kappa_- M} |A_{\kappa_+ \kappa_- M}|^2, \tag{13}$$

⁷ M. E. Rose, *Relativistic Electron Theory* (John Wiley & Sons, Inc., New York, 1961). Note Chap. 32.

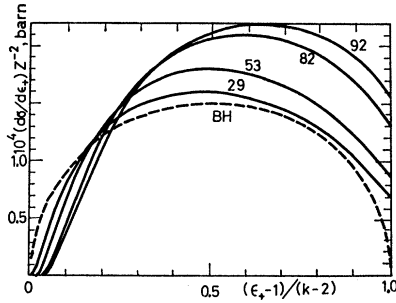


FIG. 2. Same as Fig. 1 except that the photon energy is 2.56 MeV ($k=5.00$).

η_{\pm} is defined by

$$e^{2i\eta_{\pm}} = \frac{\kappa_{\pm} - i(\gamma_{\pm}/\epsilon_{\pm})}{\gamma_{\pm} + i\eta_{\pm}}, \quad x_{\pm} = 2p_{\pm}/(k + p_{+} + p_{-}),$$

$C_{l_L l_M; M_0}$ is the Clebsch-Gordan coefficient, and F_2 is the hypergeometric function of two variables⁸ (Appell function).

Equation (13) has been obtained from the differential pair-production cross section, Eq. (3), by integration over angles.⁹ Differential cross sections, also including polarization dependences, may be obtained in the same way.

The positron spectrum was obtained by numerical evaluation⁹ of Eq. (13). The total pair-production cross section,

$$\sigma = \int \frac{d\sigma}{d\epsilon_{+}} d\epsilon_{+},$$

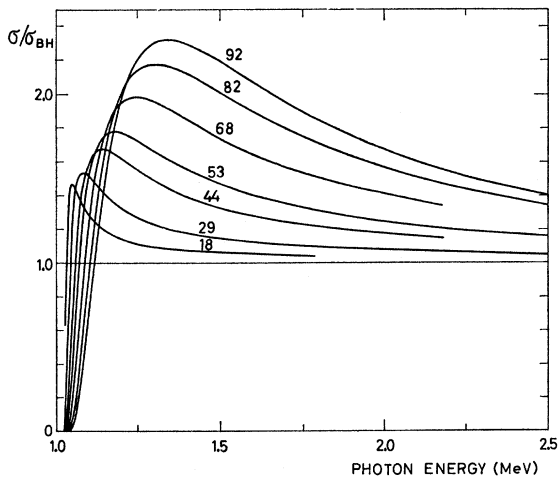


FIG. 3. Total pair-production cross section, in units of the Bethe-Heitler cross section, as a function of the photon energy. The numbers attached to the curves give the atomic number of the target element.

⁸ P. Appell and J. Kampé de Fériet, *Fonctions Hypergéométriques et Hypersphériques* (Gauthier-Villars, Paris, 1926).

⁹ For more detailed results, together with details regarding numerical calculations, see I. Øverbø (to be published).

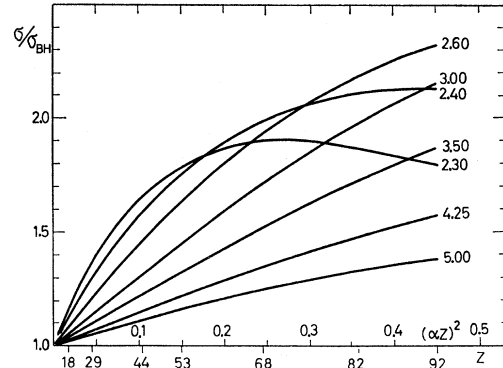


FIG. 4. Total pair-production cross section, in units of the Bethe-Heitler cross section, as a function of the atomic number of the target element. The numbers attached to the curves give the values of k in units of mc^2 .

was obtained by numerical integration of the pair spectrum.

III. RESULTS

The positron spectra for two energies, one close to the threshold, the other far away from the threshold, are shown in Figs. 1 and 2.¹⁰ The deviations from the Bethe-Heitler spectrum are considerable. As expected, the positrons are repelled by the nucleus; there are, for a given photon energy, more positrons of higher energies than predicted by the Bethe-Heitler theory.

The total pair-production cross section in units of the Bethe-Heitler cross section σ_{BH} is shown in Fig. 3 for several elements for photon energies up to 2.5 MeV. In Fig. 4, the ratio $\sigma/\sigma_{\text{BH}}$ is given as a function of $(\alpha Z)^2$. It is clear from this figure that, for increasing photon energy in the present energy range, the cross section tends towards the Z dependence

$$\sigma = \sigma_{\text{BH}}(1 + \text{const} \times Z^2),$$

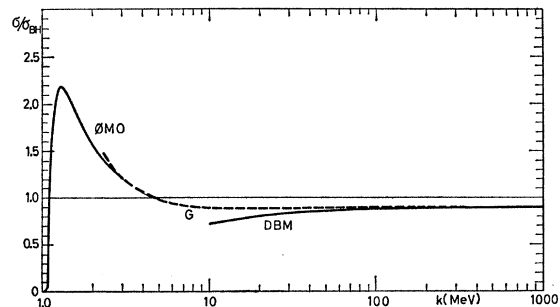


FIG. 5. Total pair-production cross section for lead, in units of the Bethe-Heitler cross section. The curves for DBM, the Davies-Bethe-Maximon results; ØMO, present results; G, modified Grodstein semiempirical formula, Eq. (14).

¹⁰ Electron spectra are obtained by replacing ϵ_{+} by $\omega - \epsilon_{+}$ in Figs. 1 and 2.

TABLE I. Comparison of Jaeger and Hulme's (JH) results^a with present (\emptyset MO) results.

ω (mc^2)	σ (barns)	Z				Error (%)
		50	54	65	82	
3.0	JH	0.17		0.34	0.67	5
	\emptyset MO	0.177		0.353	0.671	0.5
5.0	JH		1.1		3.0	10
	\emptyset MO		1.16		3.18	1
5.2	JH				3.1	10
	\emptyset MO				3.40	1

^a References 3, 4.

as has been observed experimentally several times previously.

In Table I, we have compared our results with the results obtained by Jaeger and Hulme³ and Jaeger,⁴ which were obtained in essentially the same way as were our results. The agreement is satisfactory and always within the uncertainty limits.

In Table II, the available experimental results for the total pair-production cross section¹¹⁻¹⁵ for photon energies up to 2.6 MeV are compared with the present theoretical calculation. The agreement is very good. With the ratio of cross sections ($\sigma/\sigma_{\text{BH}}$) ranging between 1.0 and 2.2, the deviation between theory and experiment is never much larger than 10%. This agreement suggests that screening effects should not be very important in the energy region considered here; the average value for all elements and energies in Table II, $\sigma_{\text{expt}}/\sigma_{\text{theory}}=0.95\pm 0.04$, might suggest an effect of screening on the cross section of the order of a few percent.

In Fig. 5, we give, for the case of lead, the Davies-Bethe-Maximon high-energy results,¹ together with the

¹¹ H. I. West, Phys. Rev. **101**, 915 (1956).¹² I. E. Dayton, Phys. Rev. **89**, 544 (1953).¹³ P. Schmid and P. Huber, Helv. Phys. Acta **27**, 152 (1954).¹⁴ B. Hahn, E. Baldinger, and P. Huber, Helv. Phys. Acta **25**, 505 (1952).¹⁵ F. Titus and A. J. Levy, Nucl. Phys. **80**, 588 (1966).

TABLE II. Comparison of theory with experimental results.

ω (MeV)	Z	$(\sigma/\sigma_{\text{BH}})_{\text{expt}}$	Ref.	$(\sigma/\sigma_{\text{BH}})_{\text{theory}}$	$\sigma_{\text{expt}}/\sigma_{\text{theory}}$	
1.173	6(C)	1.19 \pm 0.05	11	1.026	1.16 \pm 0.05	
	53(I)	1.79 \pm 0.07	11	1.780	1.005 \pm 0.04	
1.28	13(Al)	0.997 \pm 0.05	12	1.05	0.95 \pm 0.05	
	29(Cu)	1.111 \pm 0.05	12	1.244	0.89 \pm 0.04	
	29	1.18 \pm 0.14	13		0.95 \pm 0.12	
	50(Sn)	1.494 \pm 0.06	12	1.625	0.92 \pm 0.04	
	50	1.38 \pm 0.07	13		0.85 \pm 0.04	
	82(Pb)	2.04 \pm 0.06	12	2.179	0.95 \pm 0.03	
	82	2.02 \pm 0.06	13		0.93 \pm 0.03	
	82	2.08 \pm 0.22	14		0.96 \pm 0.10	
	1.333	6	1.01 \pm 0.03	11	1.010	1.00 \pm 0.03
	53	1.46 \pm 0.04	11	1.620	0.90 \pm 0.03	
1.76	82	1.58 \pm 0.05	14	1.719	0.92 \pm 0.03	
2.62	4(Be)	1.075 \pm 0.04	12	1.001	1.074 \pm 0.04	
	6	0.934 \pm 0.03	12	1.002	0.932 \pm 0.03	
	13	1.006 \pm 0.002	12	1.009	0.996 \pm 0.002	
	13	0.92 \pm 0.002	15		0.91 \pm 0.002	
	29	1.03 \pm 0.02	12	1.047	0.98 \pm 0.02	
	50	1.081 \pm 0.02	12	1.130	0.96 \pm 0.02	
	50	1.04 \pm 0.06	15		0.92 \pm 0.05	
	82	1.229 \pm 0.025	12	1.304	0.95 \pm 0.02	
	82	1.33 \pm 0.03	12		1.02 \pm 0.02	

results of the present calculation up to a photon energy of 3 MeV. We also include a simple modification of the semiempirical cross section given by Grodstein,¹⁶ which here is taken to be

$$\sigma = \sigma_{\text{BH}} - \Delta\sigma_e + (b^2/k) \ln(k-0.75), \quad (14)$$

where $\Delta\sigma_e$ is the Davies-Bethe-Maximon correction taken at infinite photon energy and b is an empirical constant. For lead, $\Delta\sigma_e=4.02$ b and $b^2=16.8$ b. Our formula, Eq. (14), differs from that of Grodstein only in that the term $\ln k$ has been replaced by $\ln(k-0.75)$. In this form, the formula agrees well with experimental results down to 3-MeV photon energy, and it connects well to the calculated cross section at 3 MeV as seen from Fig. 5.

¹⁶ G. White Grodstein, Natl. Bur. Std. (U. S.) Circ. **583**, 1 (1957).